NANO LETTERS

pubs.acs.org/NanoLett

Letter

Enhanced Nonlinear Light Generation in Oligomers of Silicon Nanoparticles under Vector Beam Illumination

Maria K. Kroychuk, Alexander S. Shorokhov, Damir F. Yagudin, Daniil A. Shilkin, Daria A. Smirnova, Irina Volkovskaya, Maxim R. Shcherbakov, Gennady Shvets, and Andrey A. Fedyanin*

Cite This: *Nano Lett.* 2020, 20, 3471−3477

Read Online

ACCESS | Metrics & More | Article Recommendations | Supporting Information

ABSTRACT: All-dielectric nanoparticle oligomers have recently emerged as promising candidates for nonlinear optical applications. Their highly resonant collective modes, however, are difficult to access by linearly polarized beams due to symmetry restraints. In this paper, we propose a new way to increase the efficiency of nonlinear processes in all-dielectric oligomers by tightly focused azimuthally polarized cylindrical vector beam illumination. We demonstrate two orders enhancement of the third-harmonic generation signal, governed by a collective optical mode represented by out-of-plane magnetic dipoles. Crucially, the collective mode is characterized by strong electromagnetic field localization in the bulk of the nonlinear material. For comparison, we measure third-harmonic generation in the same oligomer pumped with linearly and radially polarized fundamental beams, which both show significantly lower harmonic output. We also provide numerical analysis to describe and characterize the observed effect. Our findings open a new route to enhance and modulate the third-harmonic generation efficiency of Mie-resonant isolated nanostructures by tailoring the polarization of the pump beam.

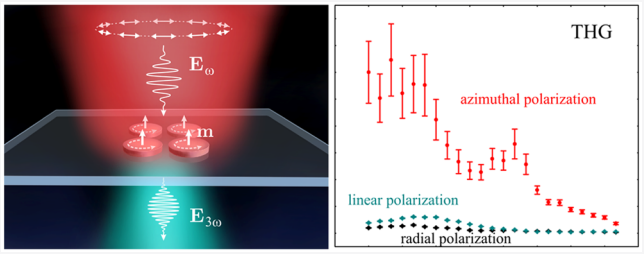

KEYWORDS: *Vector beams, azimuthal polarization, collective optical mode, third-harmonic generation, all-dielectric oligomer*

INTRODUCTION

All-dielectric nanostructures have recently gained popularity as a promising framework for nonlinear nanophotonics.[1,2] Nanostructures based on high-index dielectric nanoparticles, with optical response governed by multipolar Mie-type resonances,[3,4] proved to enhance the efficiency of nonlinear optical (NLO) effects.[5] Strong local field confinement in their volume at the magnetic dipolar resonance (MDR) excitation, as well as low losses and high stability under intense laser radiation, make them attractive for NLO applications. Single resonant dielectric nanoparticles,[6−9] metasurfaces,[10−14] and hybrid metal−dielectric systems[15−17] improved various infrared-to-visible conversion processes, avoiding the downside of phase mismatch between the pump and the harmonic waves.

Combining dielectric particles in isolated oligomers—clusters of closely located nanostructures—leads to the formation of collective optical modes[18] governed by the near-field coupling between the constituent elements of the system. Their response, both in the near-field and far-field, results in asymmetric spectral features in linear[19−21] and NLO[22,23] response due to the mode interference, as well as in nonlinear anisotropy.[24,25] However, these effects have only been demonstrated using linearly polarized Gaussian beam excitation.

Collective magnetic optical modes are known to significantly increase the efficiency of nonlinear optical effects in clusters of nanoparticles, which has been previously shown for an array of oligomers pumped under oblique incidence.[23] In the case of a single oligomer, it is symmetry-forbidden to excite such modes with linearly polarized beams under normal incidence. Under normal incidence, selective excitation of optical modes in nanoparticles and nanoparticle oligomers[26−28] can be achieved by cylindrical vector beams (CVBs)[29] with azimuthal or radial polarization. Separate control over the induced electric and magnetic dipolar modes can result in, for example, directional scattering[30−33] and dark mode formation.[34−36] The modes excited by CVBs also reveal themselves in efficient harmonics generation that has been experimentally demonstrated for individual Mie-resonant nanoparticles,[37−39] plasmonic oligomers consisting of metal nanorods with different spatial symmetries,[40] and plasmonic Fano structures.[41] However, the excitation of collective optical modes in isolated all-dielectric oligomers by structured light for enhancement of the nonlinear optical effects has not been experimentally and numerically studied so far.

Received: January 29, 2020
Revised: April 20, 2020
Published: April 23, 2020

https://dx.doi.org/10.1021/acs.nanolett.0c00393
Nano Lett. 2020, 20, 3471−3477

In this work, we apply recently developed concepts of the harmonic generation microscopy with linear, azimuthal, and radial polarized beams for investigation of individual nanoclusters and observe the collective magnetic optical mode excitation leading to an increase of the third-harmonic generation (THG) efficiency from an isolated amorphous silicon (a-Si) nanoparticle oligomer. By tailoring the polarization of the fundamental beam, we modify the third-harmonic (TH) intensity spectra of a single oligomer by selectively exciting various collective modes in the system under normal incidence. When generated by an azimuthally polarized beam, the THG from an individual a-Si nanocluster is enhanced by a factor of 120 with respect to an unstructured a-Si film of the same thickness, whereas the linearly and radially polarized beams have significantly lower yield. We support our experimental data by a modal analysis and fullwave numerical simulations.

RESULTS AND DISCUSSION

The idea of harmonic generation mapping of the sample with an azimuthally polarized beam for the THG enhancement is illustrated in Figure 1. A quadrumer of nanoparticles—four

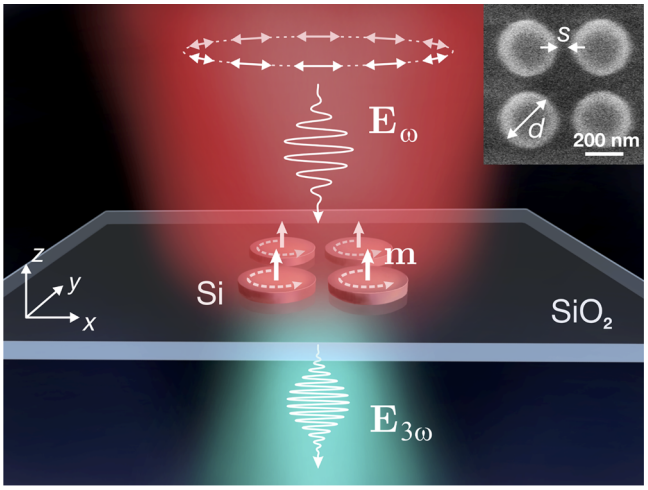

Figure 1. Sample under study and idea. Schematic representation of the oligomer collective mode excitation with AB leading to the TH intensity enhancement. Inset shows a scanning electron microscope image of an a-Si quadrumer; spacings between nanodisks are $s = 82 \pm 4$ nm, and diameters are $d = 281 \pm 4$ nm.

silicon nanodisks arranged in the vertices of a square (Figure 1, inset)—is illuminated by a normally incident tightly focused infrared femtosecond laser beam with a pulse duration of 140 fs, a spectral width of 10 nm, and a central wavelength tunable from 930 to 1050 nm. The TH light radiated from the sample is detected for various pump beam polarizations—azimuthally and radially polarized CVBs (AB and RB, respectively) and linearly polarized Gaussian beam (LB). Varying the polarization of the pump beam, one can tailor the type of excited intrinsic modes of oligomers and thus modify the local field distribution inside the cluster characterized by the localization factor $L(\omega)$. The maximum TH power corresponds to the largest $L(\omega)$ because the TH polarization source $P(3\omega)$ is proportional to the localization factor cubed:[42] $P(3\omega) \sim \hat{\chi}^{(3)}(3\omega)E(\omega)^3L(\omega)^3L(3\omega)$, where $E(\omega)$ is the pump field, $\hat{\chi}^{(3)}$ is the nonlinear polarizability tensor, and $L(3\omega)$ is the localization factor at the TH frequency, which is nonresonant in our case. Strictly speaking, for resonant nanostructures, this expression must take into account the nonuniform electric field distribution inside the volume of the particles and other factors, such as TH absorption and retardance of the point sources when calculating the far-field emission patterns. These effects, however, are fully implemented in our full-wave modeling. As shown in Figure 1, collective out-of-plane magnetic dipoles ($\mathbf{m}$) are excited when the quadrumer is pumped by a normally incident AB that results in a multifold TH intensity enhancement.

In our study, we employ isolated quadrumers: the distance between the nanoclusters $T = 10$ μm prevails over the diameter of the pump beam, which is approximately 2.5 μm (Figure 1). The samples under study were made from a film of hydrogenated a-Si with the thickness of 260 ± 5 nm deposited on a fused silica substrate. According to the scanning electron microscope images, the spacing between nanodisks equals $s = 82 \pm 4$ nm and the diameter equals $d = 281 \pm 4$ nm.

To validate our idea, we perform numerical modeling of the oligomer's scattering spectrum for various illumination conditions using the finite element method (FEM) in COMSOL Multiphysics; see Figure 2. The scattering spectra of the oligomer illuminated by AB or RB beams shown in Figure 2a noticeably differ from the one acquired by LB excitation. The difference in the spectral response can be explained by selective coupling of the pump to different modes of quadrumers. We discuss this in more detail below and in Supporting Information, section 5. For the RB, the calculated scattering cross section does not exhibit any resonance in the chosen spectral range, whereas two peaks marked as AP_1 and AP_2 arise for the AB. Figure 2b illustrates that the numerically computed linear scattering of AB is rotationally symmetric and bears multipoles of the magnetic type with $m = 0$, where m is the azimuthal index. The numerically retrieved spectrum of eigenmodes in the quadrumer, their quality factors, and near-field spatial profiles are presented in Figure 2c. We specifically identify the modes that, by symmetry, can be selectively excited by AB, RB, and LB, carrying distinct combinations of field components: (E_φ; H_r, H_z), (H_φ; E_r, E_z), (E_x, H_y), respectively. The modes were characterized by their multipolar decompositions over the spherical harmonics distinguished by azimuthal m and orbital l indices, as illustrated in Figure 2d. To achieve efficient coupling to the mode, multipolar composition of the pump source should match the multipolar structure of this mode. The strongest THG is expected in the case of efficient excitation of the mode with the highest quality factor. RP modes, including a toroidal dipole excitation RP_1, do not fall in the experimentally accessible range. The quality factor of the AP_2 mode ($Q_{AP_2} = 35$) exceeds the quality factors of the AP_1 and LP modes ($Q_{AP_1} \approx 10$ and $Q_{LP} \approx 6$); see Figure 2c. Remarkably, AB can be used to couple to the high-quality mode AP_2 most efficiently because it can be decomposed into solely magnetic multipoles with $m = 0$, maximizing the modal overlap. Although AP_2 can be interpreted as a superposition of an azimuthally symmetric magnetic dipole (MD), 72%, and a magnetic octupole (MO), 28%, AP_1 is predominantly constituted by the magnetic quadrupole (MQ); see Figure 2d. More information about the calculation of percentage composition of the modes is given in the Supporting Information, section 6. Both of these modes can be selectively addressed by AB. In turn, the LP plane wave contains

https://dx.doi.org/10.1021/acs.nanolett.0c00393
Nano Lett. 2020, 20, 3471−3477

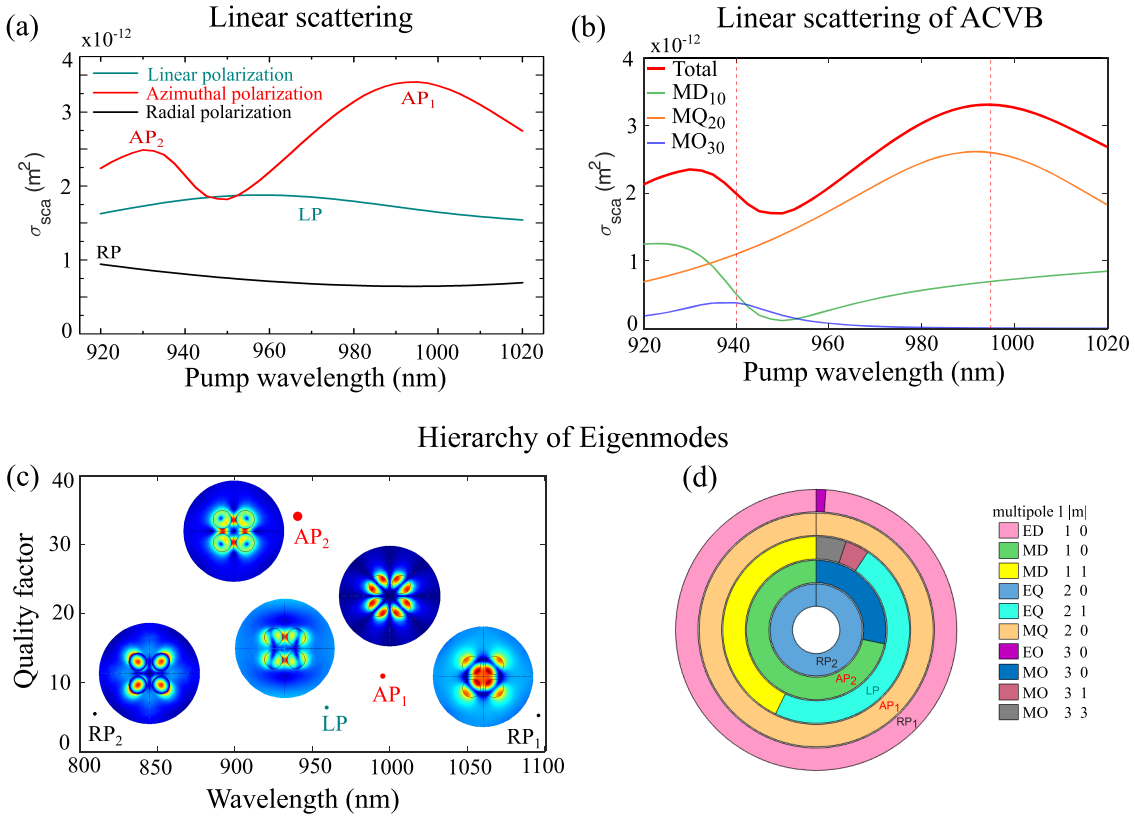

Figure 2. Linear optical response of the quadrumer. (a) Scattering cross section spectra for the quadrumer of a-Si nanodisks for LB (green curve), AB (red curve), and RB (black curve) illumination at normal incidence. (b) Multipolar decomposition of AB linear scattering featuring magnetic multipoles with $m = 0$. Vertical red dashed lines mark the AP_1 and AP_2 eigenmode wavelengths. (c) Quality factors and wavelengths of the modes in the quadrumer of a-Si nanodisks. Insets: Near-field distributions (shown is the electric field norm at the disks midheight in the *xy* cross section, which is parallel to the sample plane). (d) Multipolar decompositions of the collective eigenmodes (indicated as LP, $RP_{1,2}$, $AP_{1,2}$) in the quadrumer.

multipoles exclusively with $m = \pm 1$ and couples only to LP mode possessing a nonzero net in-plane MD.

The resonant excitation of the modes can be traced back in the spectral features of linear scattering plotted in Figure 2a, and it is also reflected in the numerically simulated electric field distribution under AB, LB, and RB excitations (see Supporting Information, Figure S3). In the LP and AP_1 regions, nanodisks behave as in-plane magnetic dipoles being *y*-aligned for LP and 90° rotated for AP_1, resembling the field structure of the pump beam. The AP_2 mode is related to the out-of-plane magnetic dipoles (OMD) resonantly excited by H_z component of the AB in each nanodisk of the quadrumer. The field is mostly confined in the bulk of nanoparticles. Note that the nanoparticle aspect ratio and the spacing between them can be varied to tune the spectral position of the AP_2 mode (see Supporting Information, section 2). It is not uncommon to observe asymmetric features in the scattering spectra of oligomers due to Fano interferences.[19,23] In our case, the modes are excited selectively, prohibiting intermodal interference and resulting in symmetric Lorentzian spectral lines.

We optically characterized the quadrumer presented in the inset of Figure 1 by linear scattering spectroscopy under LB excitation (Figure 3a, green curve) using dark-field single-particle scattering spectroscopy (see Supporting Information, section 3). White light was sent to a field stop, whose image was formed at the sample plane from the air side (see Supporting Information, Figure S7). The scattered light was spatially filtered by a central stop that blocked the forward illumination. A clear peak at $\lambda = 960$ nm, marked as LP, shown in Figure 2a, can be attributed to the excitation of MDR in the disks constituting the quadrumer.

By using a home-built THG microscopy apparatus, with its main part schematically presented in Supporting Information Figure S8a, we measured the TH intensity spectra of the oligomer for various illumination conditions (LB, AB, and RB). The polarization type of the pump beam was controlled by a liquid crystal ARCoptix polarizer (LCP) that converted LB into AB or RB.[43] The chosen beam was focused in a 2.5 μm wide spot on the sample by an objective lens with a high NA of 0.85. The output transmitted light was collected by an objective lens with an NA of 0.65 and filtered out by a color glass filter. The TH radiation was detected with a photomultiplier assembly connected to a lock-in amplifier. The position of the sample was automatically controlled in three perpendicular directions between the objective lenses that allows obtaining TH images of the oligomer (see Supporting Information, section 4, Figure S8b,c). For each spectral point, we averaged the TH intensity over five consecutive measurements and divided the TH intensity from the quadrumer by the TH intensity of an unstructured a-Si film measured under the same experimental conditions. After receiving the full spectrum, the procedure was repeated three times. The resulting spectra are the arithmetic mean of the latter. All results presented below were obtained without taking into account the difference in the volume of the nonlinear material between the samples and the film, a factor of about 13. However, the difference in the volume of excited material does

https://dx.doi.org/10.1021/acs.nanolett.0c00393
Nano Lett. 2020, 20, 3471−3477

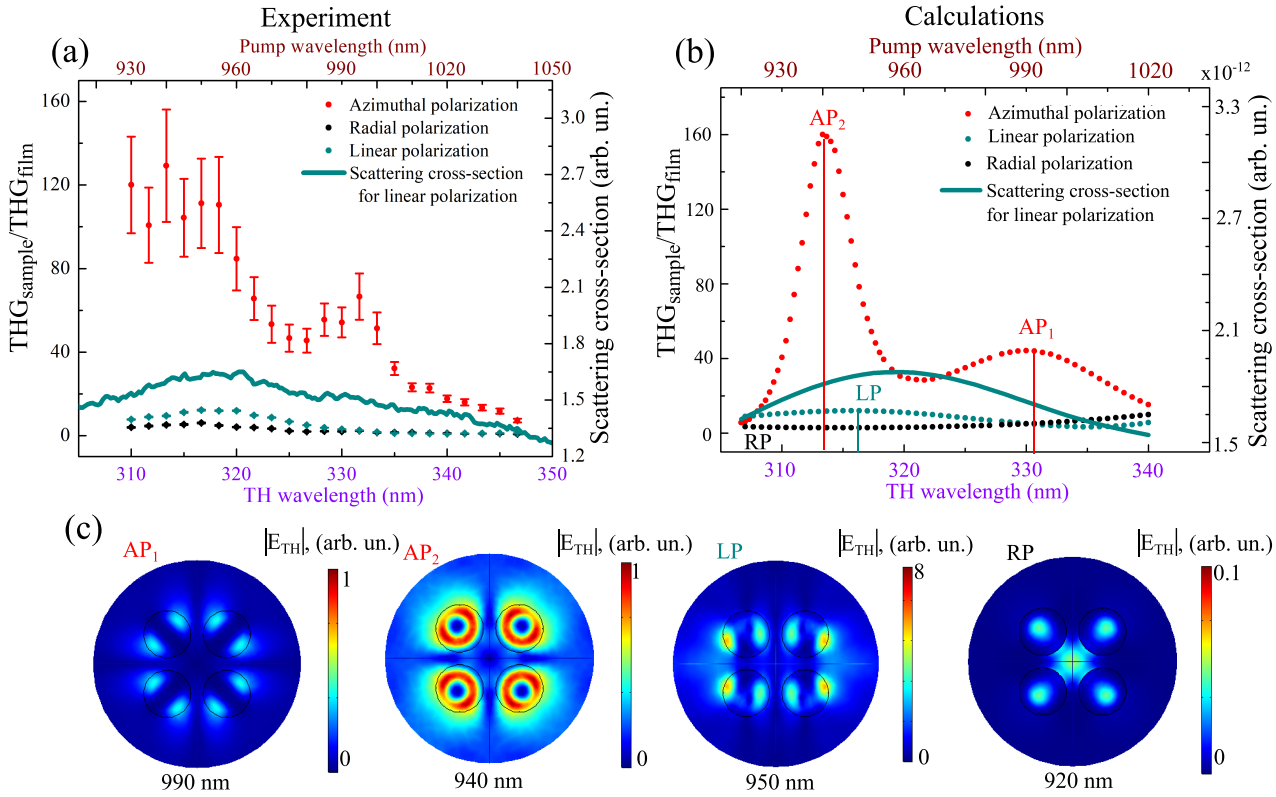

Figure 3. Nonlinear optical response of the quadrumer. (a) Experimental TH intensity spectra for the quadrumer of a-Si nanodisks normalized to the TH intensity from an unstructured a-Si film for LB (green dots), AB (red dots), and RB (black dots) illumination at normal incidence. Green curve indicates experimental scattering cross section for the quadrumer of a-Si nanodisks for LB illumination at normal incidence. (b) Normalized numerical TH intensity spectra for the quadrumer of a-Si nanodisks for LB (green dots), AB (red dots), and RB (black dots) illumination at normal incidence. Green curve indicates numerical scattering cross section spectra for the quadrumer of a-Si nanodisks for LB illumination at normal incidence. (c) Simulated electric near-field distributions at the TH wavelength corresponding to the specific points in the scattering cross section spectra: AP_1 indicates the wavelength of the oligomer MQR under AB excitation, AP_2 stands for the OMD mode under AB excitation, LP stands for the MDR of the oligomer under LB excitation, and RP stands for the electric field distribution for RB.

not affect the TH differences for various pump beam polarizations, which is mainly in the focus of the work. The maximum of the normalized TH output was observed when the center of the pump beam coincided with the center of the oligomer. For more information about the experiment setup and conditions, see Supporting Information, section 4.

Figure 3a presents the measured TH power spectra of the quadrumer for the AB, RB, and LB excitation. As predicted by the local field analysis, no valuable TH power enhancement was observed for RB (Figure 3a, black dots) even in the spectral vicinity of MDR (λ = 960 nm). The pump polarization direction was kept at approximately 20° with respect to the side of the quadrumer for the LB excitation. This alignment is chosen to get the highest possible TH intensity in the LB case, in accord with our previous findings.[25] A 12-fold THG enhancement compared to the unstructured a-Si film is obtained for such experimental conditions (Figure 3a, green dots), for pumping at λ = 950 nm, which corresponds to the MDR excitation with good accuracy. Taking into account the TH intensity modulation described in ref 25, the maximum THG enhancement obtained for polarization parallel to the diagonal of oligomer can be further enhanced by approximately 15%. When the illumination wavelength is far from the MDR, the TH intensities for LB and RB are nearly the same and tend to zero. The red dots in Figure 3a show the TH intensity enhancement spectrum for the same quadrumer pumped by the AB. The vertical red bars on the spectrum indicate the systematic and statistical errors. Two peaks are identified in the spectrum with the resonances at about λ_1 = 940 nm and λ_2 = 990 nm. According to the electric field distribution analysis at the TH wavelength (Figure 3c), λ_1 is associated with the OMD mode excitation (AP_2 point in Figures 2a and 3b) and manifests itself in the 120-fold enhancement in the TH conversion efficiency compared to that of the unstructured silicon film; λ_2 corresponds to the MQ resonance of the quadrumer under AB pumping (AP_1 point in Figures 2b and 3b) and is accompanied by the 65-fold signal gain comparing to the unstructured a-Si film. The overall maximum of the TH signal is experimentally observed for the OMD mode, where the normalized TH intensity is twice the TH signal at the MQR under the AB excitation and exceeds the TH power at the MDR under the LB excitation by 2 orders of magnitude.

We confirm our experimental results by numerical modeling of the THG using FEM technique. The results are shown in Figure 3b and can be understood in the following way. The nonlinear source inside each particle is driven by the magnetic resonance[1] and is roughly proportional to the magnetic dipole moment cubed, $\propto|\mathbf{m}_i^3(\omega)|$. For the LB pumping, the optical response of the oligomer is mostly governed by the in-plane magnetic dipoles resonantly excited in each silicon disk at the MDR wavelength (Figure 3c, LP), and the overall dipole moment of the system differs from zero, which results in one peak in the TH spectrum (Figure 3b, green curve) with a slight blue shift from the MDR wavelength in the linear scattering

https://dx.doi.org/10.1021/acs.nanolett.0c00393
Nano Lett. 2020, 20, 3471−3477

spectrum (Figure 3b, green dots). When the quadrumer is irradiated with the AB, there are two modes excited in the oligomer, which respectively lead to two maxima in the TH spectrum—AP_1 and AP_2 (Figure 3b, red line). The collective mode indicated as AP_1 consists of radial in-plane magnetic dipoles excited by the radial part of the incident magnetic field (Figure 3c, AP_1). The second one, noted as AP_2, is governed by the out-of-plane magnetic dipoles excited by the z-part of the magnetic field and resulted in the greater quality factor of the mode and thus higher THG (Figure 3c, AP_2). A small shift of the central TH resonances wavelengths observed with respect to the peaks in the scattering cross section can be attributed both to the dispersion of a-Si at the TH wavelength and to the fact that the local fields are not necessarily at their maximum at the scattering peak.[44−46] However, the collective modes excited in the oligomers manifest themselves in both nonlinear and linear responses. At the wavelength of the AP_2 mode, the TH intensity is 2 orders of magnitude larger than the maximum under LB illumination and 4 times larger compared to that in the AP_1 mode, which agrees well with the experimental results. When the quadrumer is illuminated with the RB, the azimuthal in-plane nonresonant magnetic dipoles are excited (Figure 3c, RP), but the absence of the corresponding modes in the chosen spectral window results in a significantly weaker TH response (Figure 3b, RP). Some discrepancies between experimental and numerical results can be attributed to the possible difference of beam focusing conditions in the experiment and simulation.

We performed calculations for an individual nanodisk of the same size as in the cluster under study; see Figure S5 (Supporting Information, section 2). The TH intensity for a quadrumer was more than 80 times that of the nanodisk. It proves that specifically the selective excitation of the collective mode drives significant boost of the nonlinear optical response of the system.

CONCLUSION

To summarize, we have numerically predicted and experimentally observed the excitation of the collective out-of-plane magnetic dipole mode in an all-dielectric nanoparticle oligomer by normally incident azimuthally polarized cylindrical vector beams. The collective mode manifests itself in a more than 2 orders of magnitude (120 times) third-harmonic intensity enhancement in comparison with an unstructured a-Si film. We have demonstrated up to 2-fold modulation of the sample nonlinear output when changing the pump wavelength from the magnetic quadrupolar resonance to the out-of-plane magnetic dipolar mode wavelength for the azimuthally polarized cylindrical vector beam, which we deem a powerful way to distinguish these modes in the far-field. Moreover, we experimentally and numerically present a 2 orders of magnitude enhancement of the third-harmonic conversion efficiency when replacing a linearly polarized Gaussian beam with the azimuthally polarized cylindrical vector beam excitation. This work opens a new route to control and modulate nonlinear response of Mie-resonant isolated nanostructures by tailoring their excitation conditions.

ASSOCIATED CONTENT

Supporting Information

The Supporting Information is available free of charge at https://pubs.acs.org/doi/10.1021/acs.nanolett.0c00393.

Detailed description of the sample fabrication technique, experimental methods, and numerical modeling (PDF)

AUTHOR INFORMATION

Corresponding Author

Andrey A. Fedyanin − *Faculty of Physics, Lomonosov Moscow State University, Moscow 119991, Russia;* orcid.org/0000-0003-4708-6895; Email: fedyanin@nanolab.phys.msu.ru

Authors

Maria K. Kroychuk − *Faculty of Physics, Lomonosov Moscow State University, Moscow 119991, Russia*

Alexander S. Shorokhov − *Faculty of Physics, Lomonosov Moscow State University, Moscow 119991, Russia;* orcid.org/0000-0001-8415-2623

Damir F. Yagudin − *Faculty of Physics, Lomonosov Moscow State University, Moscow 119991, Russia*

Daniil A. Shilkin − *Faculty of Physics, Lomonosov Moscow State University, Moscow 119991, Russia*

Daria A. Smirnova − *Nonlinear Physics Centre, Australian National University, Canberra, ACT 2601, Australia; Institute of Applied Physics, Nizhny Novgorod 603950, Russia*

Irina Volkovskaya − *Institute of Applied Physics, Nizhny Novgorod 603950, Russia*

Maxim R. Shcherbakov − *Faculty of Physics, Lomonosov Moscow State University, Moscow 119991, Russia; School of Applied and Engineering Physics, Cornell University, Ithaca, New York 14853, United States*

Gennady Shvets − *School of Applied and Engineering Physics, Cornell University, Ithaca, New York 14853, United States*

Complete contact information is available at: https://pubs.acs.org/10.1021/acs.nanolett.0c00393

Notes

The authors declare no competing financial interest.

ACKNOWLEDGMENTS

This work was performed in part at the Cornell NanoScale Facility, a member of the National Nanotechnology Coordinated Infrastructure (NNCI), which was supported by the National Science Foundation (Grant ECCS-1542081). The work was performed under financial support of the Russian Ministry of Education and Science (Grant No. 14.W03.31.0008, development of the nonlinear microscopy setup), MSU Quantum Technology Center and Foundation for the Advancement of Theoretical Physics and Mathematics "BASIS" 19-2-6-155-1 (numerical results), and the Russian Foundation for Basic Research (18-02-00880 and 19-32-90218 third-harmonic microscopy experiments). D.A.S. acknowledges funding from the Australian Research Council Early Career Researcher Award (DE190100430) and the Russian Foundation for Basic Research (Grant Nos. 18-02-00381 and 19-02-00261). I.I.V. acknowledges partial support by the Foundation for the Advancement of Theoretical Physics and Mathematics "Basis". G.S. and M.R.S. acknowledge support by the Cornell Center for Materials Research with funding from the NSF MRSEC program (DMR-1719875) and Office of Naval Research (ONR) under Grant no. N00014-17-1-2161. The authors are grateful to S. Dagesyan for the help with the SEM characterization, E. Lyubin for assistance with scattering spectroscopy, and Y. Kivshar for fruitful discussions.

REFERENCES

(1) Smirnova, D.; Kivshar, Y. S. Multipolar nonlinear nanophotonics. *Optica* **2016**, *3*, 1241−1255.
(2) Kuznetsov, A. I.; Miroshnichenko, A. E.; Brongersma, M. L.; Kivshar, Y. S.; Luk'yanchuk, B. Optically resonant dielectric nanostructures. *Science* **2016**, *354*, aag2472.
(3) Kuznetsov, A. I.; Miroshnichenko, A. E.; Fu, Y. H.; Zhang, J.; Luk'yanchuk, B. Magnetic light. *Sci. Rep.* **2012**, *2*, 492.
(4) Evlyukhin, A. B.; Novikov, S. M.; Zywietz, U.; Eriksen, R. L.; Reinhardt, C.; Bozhevolnyi, S. I.; Chichkov, B. N. Demonstration of magnetic dipole resonances of dielectric nanospheres in the visible region. *Nano Lett.* **2012**, *12*, 3749−3755.
(5) Krasnok, A.; Tymchenko, M.; Alù, A. Nonlinear metasurfaces: a paradigm shift in nonlinear optics. *Mater. Today* **2018**, *21*, 8−21.
(6) Shcherbakov, M. R.; Neshev, D. N.; Hopkins, B.; Shorokhov, A. S.; Staude, I.; Melik-Gaykazyan, E. V.; Decker, M.; Ezhov, A. A.; Miroshnichenko, A. E.; Brener, I.; Fedyanin, A. A.; Kivshar, Y. S. Enhanced third-harmonic generation in silicon nanoparticles driven by magnetic response. *Nano Lett.* **2014**, *14*, 6488−6492.
(7) Carletti, L.; Locatelli, A.; Stepanenko, O.; Leo, G.; De Angelis, C. Enhanced second-harmonic generation from magnetic resonance in AlGaAs nanoantennas. *Opt. Express* **2015**, *23*, 26544−26550.
(8) Grinblat, G.; Li, Y.; Nielsen, M. P.; Oulton, R. F.; Maier, S. A. Degenerate four-wave mixing in a multiresonant germanium nanodisk. *ACS Photonics* **2017**, *4*, 2144−2149.
(9) Makarov, S. V.; Petrov, M. I.; Zywietz, U.; Milichko, V.; Zuev, D.; Lopanitsyna, N.; Kuksin, A.; Mukhin, I.; Zograf, G.; Ubyivovk, E.; Smirnova, D.; Starikov, S.; Chichkov, B.; Kivshar, Y. Efficient second-harmonic generation in nanocrystalline silicon nanoparticles. *Nano Lett.* **2017**, *17*, 3047−3053.
(10) Kruk, S.; Poddubny, A.; Smirnova, D.; Wang, L.; Slobozhanyuk, A.; Shorokhov, A.; Kravchenko, I.; Luther-Davies, B.; Kivshar, Y. Nonlinear light generation in topological nanostructures. *Nat. Nanotechnol.* **2019**, *14*, 126.
(11) Liu, S.; Sinclair, M. B.; Saravi, S.; Keeler, G. A.; Yang, Y.; Reno, J.; Peake, G. M.; Setzpfandt, F.; Staude, I.; Pertsch, T.; Brener, I. Resonantly enhanced second-harmonic generation using III−V semiconductor all-dielectric metasurfaces. *Nano Lett.* **2016**, *16*, 5426−5432.
(12) Vabishchevich, P. P.; Liu, S.; Sinclair, M. B.; Keeler, G. A.; Peake, G. M.; Brener, I. Enhanced second-harmonic generation using broken symmetry III−V semiconductor Fano metasurfaces. *ACS Photonics* **2018**, *5*, 1685−1690.
(13) Lochner, F. J.; Fedotova, A. N.; Liu, S.; Keeler, G. A.; Peake, G. M.; Saravi, S.; Shcherbakov, M. R.; Burger, S.; Fedyanin, A. A.; Brener, I.; Pertsch, T.; Setzpfandt, F.; Staude, I. Polarization-dependent second harmonic diffraction from resonantGa As metasurfaces. *ACS Photonics* **2018**, *5*, 1786−1793.
(14) Smirnova, D.; Kruk, S.; Leykam, D.; Melik-Gaykazyan, E.; Choi, D.-Y.; Kivshar, Y. Third-harmonic generation in photonic topological metasurfaces. *Phys. Rev. Lett.* **2019**, *123*, 103901.
(15) Shibanuma, T.; Grinblat, G.; Albella, P.; Maier, S. A. Efficient third harmonic generation from metal−dielectric hybrid nanoantennas. *Nano Lett.* **2017**, *17*, 2647−2651.
(16) Linnenbank, H.; Grynko, Y.; Förstner, J.; Linden, S. Second harmonic generation spectroscopy on hybrid plasmonic/dielectric nanoantennas. *Light: Sci. Appl.* **2016**, *5*, No. e16013.
(17) Aouani, H.; Rahmani, M.; Navarro-Cía, M.; Maier, S. A. Third-harmonic-upconversion enhancement from a single semiconductor nanoparticle coupled to a plasmonic antenna. *Nat. Nanotechnol.* **2014**, *9*, 290.
(18) Hopkins, B.; Poddubny, A. N.; Miroshnichenko, A. E.; Kivshar, Y. S. Revisiting the physics of Fano resonances for nanoparticle oligomers. *Phys. Rev. A: At., Mol., Opt. Phys.* **2013**, *88*, 053819.
(19) Limonov, M. F.; Rybin, M. V.; Poddubny, A. N.; Kivshar, Y. S. Fano resonances in photonics. *Nat. Photonics* **2017**, *11*, 543.
(20) Fan, P.; Yu, Z.; Fan, S.; Brongersma, M. L. Optical Fano resonance of an individual semiconductor nanostructure. *Nat. Mater.* **2014**, *13*, 471.
(21) Chong, K. E.; Hopkins, B.; Staude, I.; Miroshnichenko, A. E.; Dominguez, J.; Decker, M.; Neshev, D. N.; Brener, I.; Kivshar, Y. S. Observation of Fano resonances in all-dielectric nanoparticle oligomers. *Small* **2014**, *10*, 1985−1990.
(22) Shcherbakov, M. R.; Shorokhov, A. S.; Neshev, D. N.; Hopkins, B.; Staude, I.; Melik-Gaykazyan, E. V.; Ezhov, A. A.; Miroshnichenko, A. E.; Brener, I.; Fedyanin, A. A.; Kivshar, Y. Nonlinear interference and tailorable third-harmonic generation from dielectric oligomers. *ACS Photonics* **2015**, *2*, 578−582.
(23) Shorokhov, A. S.; Melik-Gaykazyan, E. V.; Smirnova, D. A.; Hopkins, B.; Chong, K. E.; Choi, D.-Y.; Shcherbakov, M. R.; Miroshnichenko, A. E.; Neshev, D. N.; Fedyanin, A. A.; Kivshar, Y. S. Multifold enhancement of third-harmonic generation in dielectric nanoparticles driven by magnetic Fano resonances. *Nano Lett.* **2016**, *16*, 4857−4861.
(24) Rahmani, M.; Shorokhov, A. S.; Hopkins, B.; Miroshnichenko, A. E.; Shcherbakov, M. R.; Camacho-Morales, R.; Fedyanin, A. A.; Neshev, D. N.; Kivshar, Y. S. Nonlinear symmetry breaking in symmetric oligomers. *ACS Photonics* **2017**, *4*, 454−461.
(25) Kroychuk, M. K.; Yagudin, D. F.; Shorokhov, A. S.; Smirnova, D. A.; Volkovskaya, I. I.; Shcherbakov, M. R.; Shvets, G.; Kivshar, Y. S.; Fedyanin, A. A. Tailored Nonlinear Anisotropy in Mie-Resonant Dielectric Oligomers. *Adv. Opt. Mater.* **2019**, *7*, 1900447.
(26) Woźniak, P.; Banzer, P.; Leuchs, G. Selective switching of individual multipole resonances in single dielectric nanoparticles. *Laser & Photonics Reviews* **2015**, *9*, 231−240.
(27) Ahmadivand, A.; Sinha, R.; Pala, N. Magnetic Fano resonances in all-dielectric nanocomplexes under cylindrical vector beams excitation. *Opt. Laser Technol.* **2017**, *90*, 65−70.
(28) Yanai, A.; Grajower, M.; Lerman, G. M.; Hentschel, M.; Giessen, H.; Levy, U. Near-and far-field properties of plasmonic oligomers under radially and azimuthally polarized light excitation. *ACS Nano* **2014**, *8*, 4969−4974.
(29) Zhan, Q. Cylindrical vector beams: from mathematical concepts to applications. *Adv. Opt. Photonics* **2009**, *1*, 1−57.
(30) Xi, Z.; Wei, L.; Adam, A.; Urbach, H. Broadband active tuning of unidirectional scattering from nanoantenna using combined radially and azimuthally polarized beams. *Opt. Lett.* **2016**, *41*, 33−36.
(31) Wei, L.; Bhattacharya, N.; Urbach, H. P. Adding a spin to Kerker's condition: angular tuning of directional scattering with designed excitation. *Opt. Lett.* **2017**, *42*, 1776−1779.
(32) Neugebauer, M.; Woźniak, P.; Bag, A.; Leuchs, G.; Banzer, P. Polarization-controlled directional scattering for nanoscopic position sensing. *Nat. Commun.* **2016**, *7*, 11286.
(33) Neugebauer, M.; Bauer, T.; Banzer, P.; Leuchs, G. Polarization tailored light driven directional optical nanobeacon. *Nano Lett.* **2014**, *14*, 2546−2551.
(34) Sancho-Parramon, J.; Bosch, S. Dark modes and Fano resonances in plasmonic clusters excited by cylindrical vector beams. *ACS Nano* **2012**, *6*, 8415−8423.
(35) Das, T.; Schuller, J. A. Dark modes and field enhancements in dielectric dimers illuminated by cylindrical vector beams. *Phys. Rev. B: Condens. Matter Mater. Phys.* **2017**, *95*, 201111.
(36) Bao, Y.; Zhu, X.; Fang, Z. Plasmonic toroidal dipolar response under radially polarized excitation. *Sci. Rep.* **2015**, *5*, 11793.
(37) Turquet, L.; Kakko, J.-P.; Zang, X.; Naskali, L.; Karvonen, L.; Jiang, H.; Huhtio, T.; Kauppinen, E.; Lipsanen, H.; Kauranen, M.; Bautista, G. Tailorable second-harmonic generation from an individual nanowire using spatially phase-shaped beams. *Laser & Photonics Reviews* **2017**, *11*, 1600175.
(38) Melik-Gaykazyan, E. V.; Kruk, S. S.; Camacho-Morales, R.; Xu, L.; Rahmani, M.; Zangeneh Kamali, K.; Lamprianidis, A.; Miroshnichenko, A. E.; Fedyanin, A. A.; Neshev, D. N.; Kivshar, Y. S. Selective third-harmonic generation by structured light in Mie-resonant nanoparticles. *ACS Photonics* **2018**, *5*, 728−733.
(39) Koshelev, K.; Kruk, S.; Melik-Gaykazyan, E.; Choi, J.-H.; Bogdanov, A.; Park, H.-G.; Kivshar, Y. Subwavelength dielectric resonators for nonlinear nanophotonics. *Science* **2020**, *367*, 288−292.

https://dx.doi.org/10.1021/acs.nanolett.0c00393
Nano Lett. 2020, 20, 3471−3477

(40) Bautista, G.; Dreser, C.; Zang, X.; Kern, D. P.; Kauranen, M.; Fleischer, M. Collective Effects in Second-Harmonic Generation from Plasmonic Oligomers. *Nano Lett.* **2018**, *18*, 2571−2580.
(41) Shang, W.; Xiao, F.; Han, L.; Premaratne, M.; Mei, T.; Zhao, J. Enhanced second harmonic generation from a plasmonic Fano structure subjected to an azimuthally polarized light beam. *J. Phys.: Condens. Matter* **2018**, *30*, 064004.
(42) Shen, Y.-R. *The Principles of Nonlinear Optics*; Wiley: New York, 1984.
(43) Stalder, M.; Schadt, M. Linearly polarized light with axial symmetry generated by liquid-crystal polarization converters. *Opt. Lett.* **1996**, *21*, 1948−1950.
(44) Wang, L.; Shorokhov, A. S.; Melentiev, P. N.; Kruk, S.; Decker, M.; Helgert, C.; Setzpfandt, F.; Fedyanin, A. A.; Kivshar, Y. S.; Neshev, D. N. Multipolar third-harmonic generation in fishnet metamaterials. *ACS Photonics* **2016**, *3*, 1494−1499.
(45) Melentiev, P. N.; Afanasiev, A. E.; Kuzin, A. A.; Gusev, V. M.; Kompanets, O. N.; Esenaliev, R. O.; Balykin, V. I. Split hole resonator: A nanoscale UV light source. *Nano Lett.* **2016**, *16*, 1138−1142.
(46) Melik-Gaykazyan, E. V.; Shcherbakov, M. R.; Shorokhov, A. S.; Staude, I.; Brener, I.; Neshev, D. N.; Kivshar, Y. S.; Fedyanin, A. A. Third-harmonic generation from Mie-type resonances of isolated all-dielectric nanoparticles. *Philos. Trans. R. Soc., A* **2017**, *375*, 20160281.

https://dx.doi.org/10.1021/acs.nanolett.0c00393
Nano Lett. 2020, 20, 3471−3477